

Quasisymplectic integrators for stochastic differential equations

R. Mannella

Dipartimento di Fisica and INFN, UdR Pisa, Università degli Studi di Pisa, Via Buonarroti 2, 56100 Pisa, Italy

(Received 4 December 2003; published 30 April 2004)

Two specialized algorithms for the numerical integration of the equations of motion of a Brownian walker obeying detailed balance are introduced. The algorithms become symplectic in the appropriate limits and reproduce the equilibrium distributions to some higher order in the integration time step. Comparisons with other existing integration schemes are carried out both for static and dynamical quantities.

DOI: 10.1103/PhysRevE.69.041107

PACS number(s): 05.40.-a, 05.10.-a, 05.20.-y, 02.50.-r

I. INTRODUCTION

Stochastic processes are well known to be at the heart of many physical systems [1]. Several approaches have hence been developed to understand the dynamics which is realized given specific models: among others, one of the most used ones is Monte Carlo integration of the equations of motion.

The literature on the numerical integration of stochastic differential equations is huge: we will limit here to mention a couple of classical citations widely used in the physics community [2–4]. Additional comments and references can be found in Ref. [5]. The numerical algorithms presented in these works are general and can be applied to basically any flow; however, they might not be the optimal ones for cases when additional information about the details of the system under study are available.

An important class for which dedicated algorithms can be derived is given by the following equations of motion:

$$\dot{x} = v,$$

$$\dot{v} = -\gamma v + F(x) + \xi(t), \quad (1)$$

where $\xi(t)$ is a random Gaussian noise, with zero average and standard deviation

$$\langle \xi(t)\xi(s) \rangle = 2\gamma T\delta(t-s).$$

In the following, we will also use $V(x)$, defined as $F(x) \equiv -V'(x)$. Note that although we are dealing here with only one Brownian walker, the algorithms we are going to show can be easily extended to the case when x and v are vectors and $F_i(x)$, the force acting on the i th walker, is a function of all other walkers.

The above equation is commonly found in the liquid state literature (for numerical schemes appropriate in the integration of the Brownian dynamics of a liquid, see among others [6–13]) and some algorithms have been proposed, over the years, for its numerical integration.

To date, perhaps the most widely used algorithms for the integration of Eq. (1) are the ones derived in Ref. [6], where two algorithms have been proposed (see also references therein): we will benchmark against one of them, and to this end, we will briefly review them below. Note that the system of Eq. (1) becomes symplectic when $\gamma \rightarrow 0$ and, until some recent works [14–16], this symplectic nature was not really

exploited in deriving numerical schemes. Algorithms which also use low-order symplectic schemes as basic schemes are the ones in Refs. [11–13].

The approach we will follow is to derive numerical algorithms having in mind two requirements: (i) the algorithm should become symplectic in the deterministic, frictionless limit ($T = \gamma = 0$); and (ii) the numerical algorithm should reproduce as closely as possible the equilibrium distribution, when it is defined [i.e., for $V(x)$ bounded from below, see the following section], of the system given by Eq. (1). The requirement $T = 0$ seems redundant once $\gamma = 0$ is imposed: however [14,15,17] it is possible to have symplectic stochastic dynamics [given the structure of Eq. (1), this implies an infinite T], and we need to explicitly exclude this case. As we will see below, to the best of our knowledge, either the former or the latter requirements have been enforced in the derivation of numerical schemes, but never both of them. The algorithms introduced here will improve both the algorithms of Ref. [6] and of Ref. [16].

II. BRIEF REVIEW OF THE BENCHMARK ALGORITHMS AND SOME DEFINITIONS

To assess how well each algorithm is performing, we start from the knowledge that for $V(x)$ which are bounded from below, Eq. (1) leads to an equilibrium distribution $P(x, v)$ for the variables x and v of the form

$$P(x, v) = N \exp\{-[v^2/2 + V(x)]/T\}, \quad (2)$$

where N is a normalization constant. We are going to compare the exact theoretical equilibrium distribution to the equilibrium distribution obtained from the simulations. It is possible, in principle, to check theoretically which is the equilibrium distribution which is expected integrating using a given numerical scheme, following Ref. [18]: suppose we have a numerical scheme of the form

$$x_i(t+h) = x_i(t) + hW_i(x_i, \xi)$$

then the probability distribution of x_i satisfies the Kramers-Moyal expansion

$$P(x_i, t+h) - P(x_i, t) = \sum_{n=1}^{\infty} \sum_{x_i} \frac{\partial}{\partial x_i} \cdots \frac{\partial}{\partial x_n} K_{1, \dots, n} P(x_i, t) \quad (3)$$

with

$$K_{1, \dots, n} \equiv (-1)^n \frac{1}{n!} \langle W_{x_1} \cdots W_{x_n} \rangle_{\xi},$$

where $\langle \cdots \rangle_{\xi}$ means averaging over the noise realizations and the $K_{1, \dots, n}$ depend explicitly on the integration time step h and its powers. Equation (3) is obtained [18] from the evolution equation for $P(x, t)$,

$$P(x_i, t+h) = \left\langle \int dx_i(t) P(x_i, t) \times \Pi_i \delta(x_i(t+h) - x_i(t) - hW_i(x_i, \xi)) \right\rangle_{\xi},$$

by Taylor expanding the δ function in powers of W .

A system in detailed balance at temperature T , like the one given by Eq. (1), has some theoretical equilibrium distribution [for $V(x)$ bounded from below]. A numerical scheme, however, will in general generate an equilibrium distribution which differs from the theoretical one. Following Ref. [18], we expect that

$$P(x_i, t=\infty)_{sim} = P(x_i, \infty)_{true} \exp\left(\sum_{n=1}^{\infty} h^n S_n/T\right),$$

where P_{sim} is the equilibrium distribution generated in the simulations and P_{true} is the theoretical equilibrium distribution. Given the explicit form of the numerical scheme, the various $K_{1, \dots, n}$ can be computed: applying Eq. (3) with P_{sim} on the right-hand side (rhs) as $P(x_i, t)$, and expanding the rhs of Eq. (3) in the small parameter h , assuming (equilibrium) that $P(x_i, t+h) - P(x_i, t) = 0$, we can derive the equations satisfied by the S_i annihilating the coefficients in an h power series. Note that the lowest order in h is the “standard” Fokker-Planck equation for the system under study. The first nonzero S_i yields the correction to the true equilibrium distribution generated by the numerical scheme.

Let us show how to use Eq. (3) taking one of the algorithms of Ref. [6]. This algorithm integrates Eq. (1) using the prescription

$$\begin{aligned} x(t+h) &= x(t) + c_1 h v(t) + c_2 h^2 F(x(t)) + \eta_1, \\ v(t+h) &= c_0 v(t) + c_1 h F(x(t)) + \eta_2, \end{aligned} \quad (4)$$

where

$$c_0 = e^{-\gamma h}, \quad c_1 = \frac{1 - c_0}{\gamma h}, \quad c_2 = \frac{1 - c_1}{\gamma h},$$

and η_1 and η_2 are two random Gaussian variables with zero average and moments,

$$\langle \eta_1^2 \rangle = \frac{Th}{\gamma} \left(2 - \frac{3 - 4e^{-\gamma h} + e^{-2\gamma h}}{\gamma h} \right),$$

$$\langle \eta_2^2 \rangle = T(1 - e^{-2\gamma h}),$$

$$\langle \eta_1 \eta_2 \rangle = \frac{T}{\gamma} (1 - e^{-\gamma h})^2.$$

The algebra to derive the correction to the equilibrium distribution induced by the numerical scheme in the general case and for a given high-order integration scheme can be formidable; however, for a flow like Eq. (1) and for the scheme given by Eq. (4), the algebra is manageable. We compute first some of the lowest K 's, up to $\langle W^4 \rangle$, i.e., up to terms such as K_{ijkl} . To give a glimpse of the procedure followed, we have, for instance,

$$K_x = h v(t) - h^2 [\gamma v(t) + V'(x(t))] 2 + o(h^3),$$

$$\begin{aligned} K_{xxv} &= h[2\langle \eta_1 \eta_2 \rangle v(t) + \langle \eta_1^2 \rangle] + h^2 \{-\langle \eta_1 \eta_2 \rangle [\gamma v(t) + V'(x(t))] \\ &\quad + \langle \eta_1^2 \rangle \gamma [\gamma v(t) + V'(x(t))] / 2\} + o(h^3), \end{aligned}$$

and so on. Assuming that [see Eq. (2), with $S \equiv S_1$]

$$P(x, v) = N \exp\{-[v^2/2 + V(x) + hS(x, v)]/T\},$$

plugging the scheme of Eq. (4) into Eq. (3), using the computed expressions of K 's, we have that $S(x, v)$ satisfies the partial differential equation

$$\begin{aligned} \frac{\partial^2 S(x, v)}{\partial v^2} - \frac{v}{T\gamma} \frac{\partial S(x, v)}{\partial x} - \left(\frac{F(x)}{T\gamma} - \frac{v}{T} \right) \frac{\partial S(x, v)}{\partial v} - \frac{v^2}{2\gamma T} F'(x) \\ - \frac{1}{2\gamma} F'(x) = 0. \end{aligned}$$

This implies that this algorithm fails to reproduce the correct equilibrium distribution at $O(h)$ in the exponent. It is possible, for the case when $V(x) = \omega^2 x^2/2$, to solve this partial differential equation, obtaining the numerical equilibrium distribution at lowest order in h , which is

$$P(x, v) = N \exp\{-[v^2/2 + \omega^2 x^2/2]/\hat{T}\}$$

with

$$\hat{T} = \frac{T}{1 + \frac{\omega^2 h}{2\gamma}},$$

i.e., the numerical equilibrium distribution is similar to the correct one, but with a renormalization of the temperature. In particular, this effective temperature (the temperature “simulated” by the algorithm) goes to zero in the limit $\gamma \rightarrow 0$. In Ref. [6] it is acknowledged that the algorithm does not work well in this limit, although no formal proof is provided.

To overcome the problem with the case of small γ , in Ref. [6] a second algorithm is proposed, which reads

$$x(t+h) = x(t) + c_1 h v(t) + c_2 h^2 F(x(t)) + \eta_1,$$

$$v(t+h) = c_0 v(t) + (c_1 - c_2) h F(x(t)) + c_2 h F(x(t+h)) + \eta_2. \tag{5}$$

Using Eq. (3) to evaluate the correction to the true equilibrium distribution generated by this algorithm, we find that the contribution S_1 vanishes, and we are left with the term S_2 . In other words, this algorithm reproduces the correct equilibrium distribution at $O(h)$, but there are still corrections $O(h^2)$ in the exponent. The algorithm given in Eq. (5) is the reference algorithm which we propose to improve in the following section. We will refer to this algorithm as ‘‘Li’’ (from Liquid) in the following.

III. QUASISYMPLECTIC ALGORITHMS

A symplectic algorithm is a numerical scheme which attempts to preserve the two-forms $dq_i \times dp_i$ during the integration of a Hamiltonian flow. The quantity q_i is a generalized coordinate and p_i is the corresponding conjugate momentum. A nice introduction to the symplectic integration can be found in Refs. [19,20]. Given the Hamiltonian $H(q_i, p_i)$ and the equations of motion

$$\dot{q}_i = \{q_i, H\}, \quad \dot{p}_i = \{p_i, H\},$$

a symplectic integrator will in practice conserve some quantity \hat{H} , which in general reads

$$\hat{H} = H + h^n G(p_i, q_i),$$

where h is the integration time step and G is a function which depends on the numerical scheme used for the integration. The problem of Hamiltonian flows in the presence of fluctuations has been addressed also in Refs. [14,15], whereas quasisymplectic schemes were derived in Ref. [16] (see also below, when various comparisons are carried out). A preliminary account of the material of this section can be found in Ref. [21].

Given that we are interested here in the integration of Eq. (1), we start from the symplectic integration of Hamiltonians which are separable and quadratic in the velocities. There are very many different possible symplectic schemes: however, having in mind that we are seeking a scheme which should be used in the integration of a stochastic differential equation, we restrict ourselves to considering a scheme in the form

$$q(i) = q(i-1) + ha_i p(i-1),$$

$$p(i) = p(i-1) + hb_i F(q(i)),$$

for i between 1 and N , where $q(0) = q(t=0)$, $q(N) = q(t=h)$, etc., and h is the integration time step in the simulations. The coefficients $a(i)$ and $b(i)$ are chosen as to minimize, in some sense, the quantity $G(p, q)$.

The lowest possible symplectic algorithm one can write to integrate Eq. (1) following this approach reads, when $\gamma = T = 0$ (this scheme is also known as ‘‘leap frog’’),

$$\tilde{x} = x(t) + \frac{h}{2} v(t),$$

$$v(t+h) = v(t) + hF(\tilde{x}),$$

$$x(t+h) = \tilde{x} + \frac{h}{2} v(t+h), \tag{6}$$

where x is the position and v is the velocity. This scheme conserves the quantity $H - h^3(vFF' + v^3F''/6)/4$, where $H \equiv v^2/2 + V(x)$. It is then possible to reintroduce both the dissipation ($-\gamma v$) and the noise, writing the tentative scheme

$$\tilde{x} = x(t) + \frac{h}{2} v(t),$$

$$v(t+h) = c_2 [c_1 v(t) + hF(\tilde{x}) + d_1 \eta],$$

$$x(t+h) = \tilde{x} + \frac{h}{2} v(t+h), \tag{7}$$

where η is a Gaussian variable, with standard deviation one and average zero. We use again Eq. (3), and, imposing that the term $O(h)$ in the exponent (i.e., the term hS_1) vanishes, we find that the unknown arbitrary quantities c_1 , c_2 , and d_1 read

$$c_1 = 1 - \frac{\gamma h}{2},$$

$$c_2 = \frac{1}{1 + \gamma h/2},$$

$$d_1 = \sqrt{2T\gamma h}. \tag{8}$$

Although we will carry out more extensive comparisons further down, let us briefly compare this scheme to the scheme of Eq. (5). The present scheme is by construction well behaved in the limit of $\gamma \rightarrow 0$: it has the same accuracy in computing the equilibrium distribution as of Eq. (5); but it requires only one random deviate per integration time step [as opposed to two deviates for the scheme of Eq. (5)], so it will run faster. In the following, we will refer to the algorithm of Eq. (7) as ‘‘SLO’’ (symplectic low order).

Looking at the structure of the previous algorithm, we can try to derive an algorithm of higher order. In the derivation of Eq. (7), when we applied Eq. (3), given the number of unknown quantities we could only impose that the term $O(h)$ in the exponent disappeared. If we could somehow increase the number of unknown quantities when applying Eq. (3), while keeping the algorithm simple, we might be able to make the terms $O(h^2)$ in the exponent disappear. We start combining two steps, each one of the form of Eq. (7), done with an integration time step $h/2$,

$$x_1 = x(t) + \frac{h}{4} v(t),$$

$$v_1 = c_2 \left[c_1 v(t) + \frac{h}{2} F(x_1) + \sqrt{\gamma Th} (a_1 \eta_1 + a_2 \eta_2) \right],$$

$$\begin{aligned}
x_2 &= x_1 + \frac{h}{2}v_1, \\
v(t+h) &= c_2 \left[c_1 v_1 + \frac{h}{2}F(x_2) + \sqrt{\gamma Th}(b_1\eta_1 + b_2\eta_2) \right], \\
x(t+h) &= x_2 + \frac{h}{4}v(t+h), \tag{9}
\end{aligned}$$

where $c_1 = (1 - \gamma h/4)$ and $c_2 = 1/(1 + \gamma h/4)$. Here, η_1 and η_2 are two random Gaussian variables of standard deviation one and average zero. The idea is now to choose the coefficients a 's and b 's in such a way as to annihilate S_1 , and possibly minimize S_2 . This is done using Eq. (9) in Eq. (3), which results in a number of algebraic equations for a_i and b_i . The algebra, although straightforward, is cumbersome and we will simply report here the results. For a given a_1 , the following choice for the other three parameters will ensure that S_1 vanishes identically:

$$\begin{aligned}
b_1 &= -\frac{a_1}{7} + \frac{2\sqrt{14 - 12a_1^2}}{7}, \\
b_2 &= -\frac{(7 + 282a_1^2 + 24a_1\sqrt{14 - 16a_1^2})^{1/2}}{\sqrt{42}}, \\
a_2 &= \frac{\sqrt{42}b_2(-7\sqrt{2} + 6\sqrt{2}a_1^2 + 24a_1\sqrt{7 - 6a_1^2})}{\sqrt{3}(-14 + 588a_1^2)}.
\end{aligned}$$

As function of a_2 , we can now write the equations satisfied by S_2 : we find that S_2 vanishes for a particular choice of the parameter a_1 . Summarizing the numerics, the set of a 's and b 's which simultaneously makes S_1 and S_2 vanish is

$$\begin{aligned}
a_1 &= -1.069\ 186\ 004\ 330\ 706\ 5\dots, \\
a_2 &= -0.153\ 323\ 040\ 701\ 989\ 3\dots, \\
b_1 &= 0.304\ 491\ 312\ 885\ 406\ 5\dots, \\
b_2 &= -1.036\ 316\ 412\ 609\ 579\ 0\dots \tag{10}
\end{aligned}$$

Note that there is a symmetry: quantities with indexes 1 and 2 can be exchanged. The conclusion is that the algorithm given by Eqs. (9) and (10) is symplectic in the limit $\gamma, T \rightarrow 0$ [conserving the quantity $H - h^3(vFF' + v^3F''/6)/16$], whereas for finite γ and T it reproduces the correct equilibrium distribution with an error $O(h^3)$ in the exponent. We will refer to this algorithm as to ‘‘SHO’’ (symplectic high order).

In the following, we will use also the Heun algorithm to carry out the various comparisons. To make this paper as self-contained as possible, we recall here that the Heun algorithm for a system like the one in Eq. (1) is given by the prescription:

$$x_1 = x(t) + hv(t),$$

$$\begin{aligned}
v_1 &= v(t) - h\gamma v(t) + hF(x(t)) + \sqrt{2\gamma Th}\eta, \\
x_2 &= x(t) + hv_1, \\
v_2 &= v(t) - h\gamma v_1 + hF(x_1) + \sqrt{2\gamma Th}\eta, \\
x(t+h) &= \frac{x_1 + x_2}{2}, \quad v(t+h) = \frac{v_1 + v_2}{2}.
\end{aligned}$$

The Heun algorithm, which is a fairly widely used algorithm for the integration of generic stochastic equations, does not make use of the (quasi)symplectic nature of the flow: we expect that it will not fare too well in the limit of small γ . We recall that it is known [5] that the equilibrium distribution generated by the Heun algorithm is accurate up to $o(h^2)$ in the exponent. We will refer to the Heun scheme as to ‘‘He.’’

We will also compare our algorithms to the quasisymplectic algorithms of Ref. [16]: we should mention here that really the latter are weak integration schemes (for a definition of weak and strong integration schemes, see Ref. [2]), hence they are bound to give worse results than the other schemes when, as we do, average quantities are considered. The two algorithms considered integrate with the prescriptions (Ref. [16] should be consulted for more details):

MT1:

$$x(t+h) = x(t) + hv(t+h),$$

$$v(t+h) = v(t) - hV'(x(t+h)) - h\gamma v(t+h) + \sqrt{2Th}\gamma\eta, \tag{11}$$

where $v(t+h)$ and $x(t+h)$ should be found recursively, and

MT2:

$$\begin{aligned}
v(t+h) &= (1 - \gamma h)[v(t) - hV'(x(t)) + \sqrt{2Th}\gamma\eta], \\
x(t+h) &= x(t) + h[v(t) - hV'(x(t))]. \tag{12}
\end{aligned}$$

The random variables η take the values ± 1 . These variables are faster to generate than a Gaussian variable, hence these algorithms will run faster, allowing for a smaller integration time step to compensate for less accuracy when averaged quantities are considered. However, having said this, if we used Eq. (3) to assess these two algorithms, we would find that they both have a correction to the equilibrium distribution $O(h)$ in the exponent: these will reflect in the numerical experiments, as we will comment below.

Finally, it should be noted that given the structure of the Hamiltonian in the limit $T \rightarrow 0$, $\gamma \rightarrow 0$, which is $H = v^2/2 + V(x)$, the equilibrium distribution for Eq. (1) can also be written as

$$P(x,v) \propto \exp - H/T.$$

At first sight, it may appear that the request of a symplectic integration scheme is redundant, once we made sure that the ‘‘correct’’ equilibrium distribution is generated in the numerical integration. This is not right: the limit $T \rightarrow 0$ is singular,

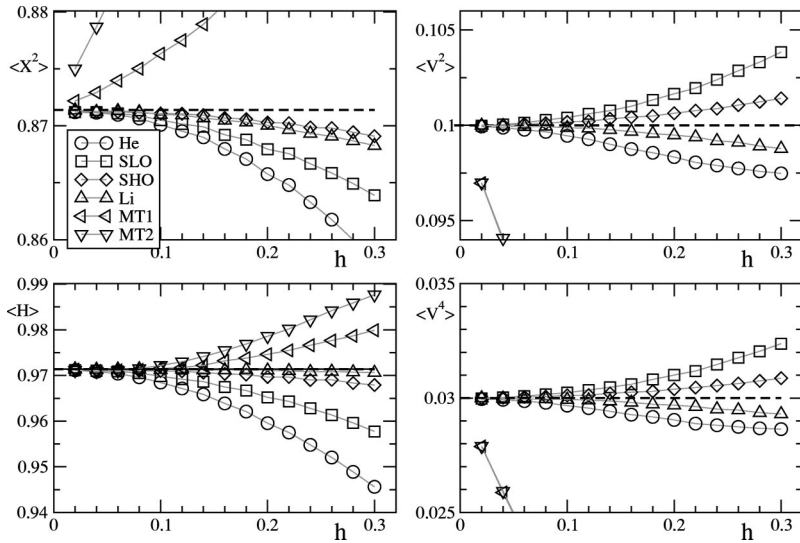


FIG. 1. Result of simulations for different integration schemes, as a function of the integration time step h , for the system in Eq. (13). Various moments are considered (see text for details), taking $T=0.1$ and $\gamma=1$. Number of averages is 4×10^7 .

hence a symplectic form for the numerical scheme when $T=0$ can (and should) be imposed as an additional condition.

IV. NUMERICAL EXPERIMENTS

We compare now the results of applying the algorithms described previously to the integration of two prototype stochastic differential equations. In all simulations, the routine used to generate uniform random variables was the subtract and carry algorithm [22,23]; for the Gaussian deviates, the appropriate uniform deviates were fed to a Ziggurath scheme [24]. Let us first consider how the different algorithms reproduce the equilibrium properties: to this end, we integrate the equations of motion and compute some equilibrium momenta, which are then compared to the theoretical ones. The averages were computed sampling the trajectories at time intervals equal to the largest time scale in the system (either $1/\gamma$ or $1/\omega$): the number of sampled points is the number of averages quoted in each figure caption. Other more conservative time scales could be considered (such as twice the largest time scale): the number of averages is so large, how-

ever, that even a factor 2 in the sampling time would make things change little. We carry out this comparison mainly to have an idea on how the algorithms perform, given that we theoretically know both the equilibrium distributions and the various moments of the systems we will consider.

The first system studied is given by

$$\dot{x} = v,$$

$$\dot{v} = -\gamma v - V'(x) + \sqrt{2\gamma T}\eta,$$

$$V(x) = x^4/4 - x^2/2. \tag{13}$$

For this system we fixed the noise intensity to $T=0.1$, and carried out the numerical integration for two different values of the damping coefficient γ and for the different integration schemes. The results are summarized in Fig. 1 (for $\gamma=1$) and in Fig. 2 (for $\gamma=10^{-2}$). The quantity $\langle H \rangle$ is defined as $\langle H \rangle \equiv \langle v^2/2 + V(x) \rangle$. In all figures, the results of the digital simulations are shown by symbols with a gray straight line as guide to the eye; the bold dashed line is the expected (theo-

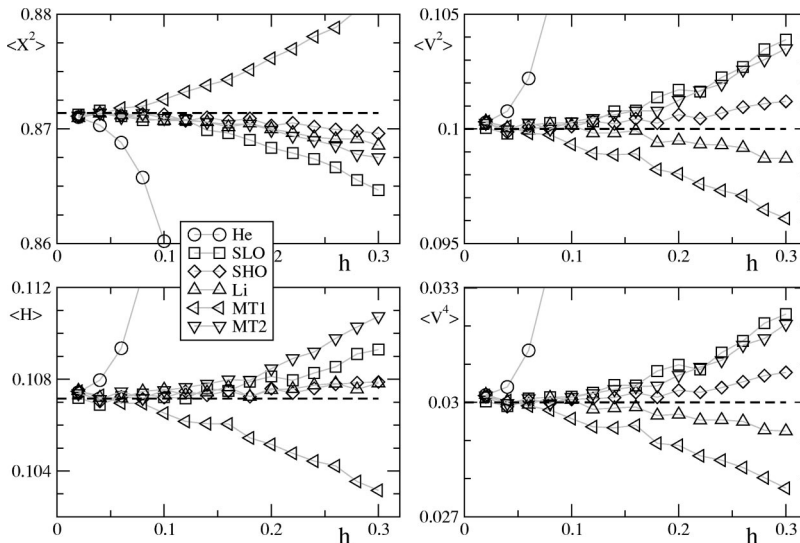


FIG. 2. Result of simulations for different integration schemes, as a function of the integration time step h , for the system in Eq. (13). Various moments are considered (see text for details), taking $T=0.1$ and $\gamma=10^{-2}$. Number of averages is 4×10^5 .

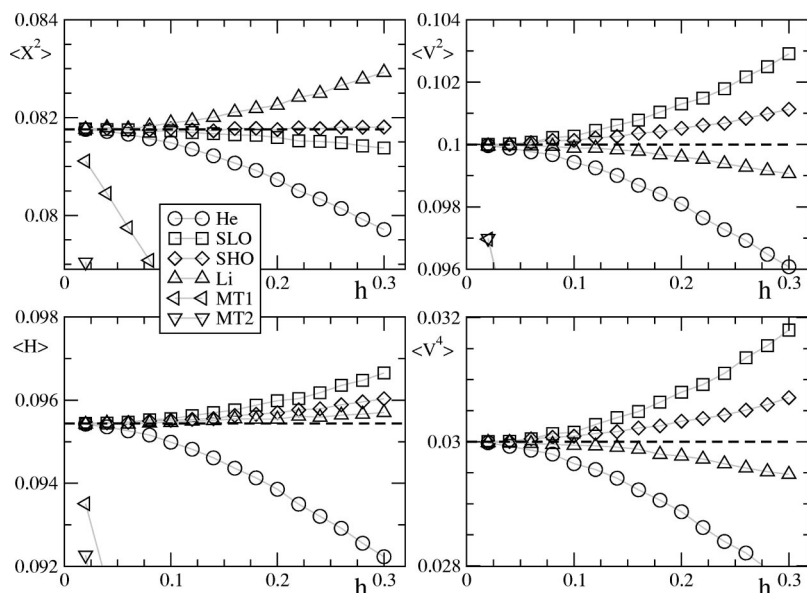


FIG. 3. Result of simulations for different integration schemes, as a function of the integration time step h , for the system in Eq. (14). Various moments are considered (see text for details), taking $T=0.1$ and $\gamma=1$. Note that the results obtained for MT1 and MT2 are outside the figure bounds, in some cases. Number of averages is 4×10^7 .

retical) value for the quantity considered. For the number of averages considered, the statistical error is much smaller than (order of) the symbols for the larger (smaller) damping.

Let us comment on the results. It is evident that the Heun method (He in figures) is not very appropriate for the smaller damping considered (Fig. 2). Even for the larger damping (Fig. 1), the Heun algorithm is typically outperformed by the SLO scheme [Eq. (7)]; note that the SLO is fairly faster than He, given that it requires only one evaluation of the deterministic force for each integration time step.

The algorithms MT1 and MT2, as expected, do not work well for the larger damping considered, and become more accurate as the damping is reduced: it should be noted that for this case, MT2 seems to be more accurate than MT1 for a given integration time step: considering that MT2 is much faster than MT1, the conclusion seems to be that MT2 ought to be preferred, between these two schemes. Note also that the error on the moments for these two schemes seems to grow linearly with the integration time step h , which is related to the $O(h)$ error in the exponent which was mentioned in the preceding section.

The Li algorithm is less accurate than SHO when the x^2 moments are considered for both values of the damping in the whole h region. The SHO is the algorithm which gives the most accurate results for the x^2 moment, and results comparable to or better than the one obtained with Li for the v^2 and v^4 moments. It is only when $\langle H \rangle$ is considered, and for the larger damping, that Li seems to be more accurate than SHO. However, care is necessary in drawing conclusions from $\langle H \rangle$: looking for instance at Fig. 1, we note that Li underestimates both v^2 and x^2 : recalling the structure of the potential $V(x) = -x^2/2 + x^4/4$, it is clear that these two underestimates tend to cancel out, leading to an $\langle H \rangle$ closer to the theoretical one, but only by virtue of a coincidental cancellation.

The second system studied is similar to the first one:

$$\dot{x} = v,$$

$$\dot{v} = -\gamma v - V'(x) + \sqrt{2\gamma T}\eta,$$

$$V(x) = x^4/4 + x^2/2, \quad (14)$$

the only difference with the system of Eq. (13) being that now the potential is monostable.

The results of the computer experiments are summarized in Figs. 3 and 4. The comments parallel the comments we already made for the system of Eq. (13). He is the least accurate scheme for small damping, although the error on the moments is quadratic on h [a signature of an $O(h^2)$ error in the equilibrium distribution]. MT1 and MT2 perform better at smaller damping, with an error on the moments which is roughly linear in the integration time step. SLO does better than both He and MT1, MT2, and for both damping considered, being as fast (if not faster) than both schemes. When the x^2 is considered, Li appears to perform worse than even SLO. SHO outperforms Li: only when H is considered, Li seems to be more accurate than SHO, but again only by virtue of a cancellation between $\langle x^2 \rangle$ and $\langle v^2 \rangle$.

We turn now to some numerical experiments to assess how the various algorithms perform when dynamical quantities are considered. These simulations are somehow more important: similar calculations, for instance, would be carried out in multistable systems to compute escape rates, for example. In most cases these quantities are not known theoretically, and stochastic simulations are one of the tools to determine them. Using the system of Eq. (13), we computed the mean first passage times (MFPTs) to go from one of the minima to the other one (the minima are located at $x = \pm 1$): the results of the simulations are summarized in Figs. 5 and 6, after averaging a suitable number of passage times between the minima. In the captions we quote a lower bound on the number of averages taken: each point was actually computed using a slightly different number of averages. Given the fairly large value of the noise intensity ($T=0.1$), there is no theory available to compute an “exact” MFPT for comparison with the simulated MFPTs. To have some refer-

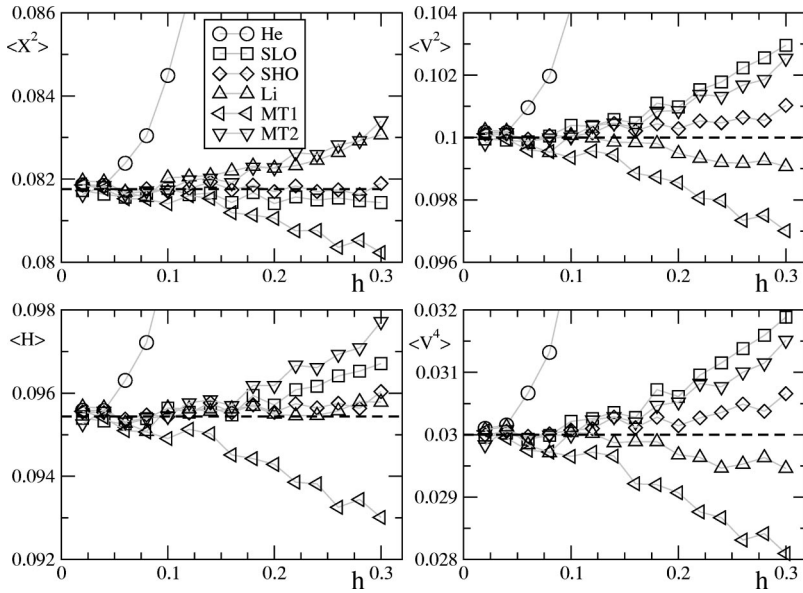


FIG. 4. Result of simulations for different integration schemes, as a function of the integration time step h , for the system in Eq. (14). Various moments are considered (see text for details), taking $T=0.1$ and $\gamma=10^{-2}$. Number of averages is 4×10^5 .

ence, we took as reference value the average of the MFPT obtained via the algorithms Li and SHO for the three smallest h values used in the simulations, and drew the dashed line at this value. For the larger damping considered (Fig. 5, $\gamma = 1$), He and SLO perform in a similar way. MT1 and MT2 give unreasonable values for the MFPT (only one point for MT1 is actually on the graph, for the smallest h considered: all other points for both algorithms are outside the MFPT range considered). Li and SHO perform in a similar way, giving results closer to the correct MFPT throughout the h range considered, with a slightly better agreement shown by SHO for larger h 's. The statistical error associated with the finiteness of the sample used is much smaller than the symbols size.

The situation is more interesting when a smaller damping is considered (Fig. 6, $\gamma=10^{-2}$). While showing an error

which grows only quadratically in h , clearly He is the algorithm which performs worse. MT1 and MT2 now give more reasonable results, and they yield MFPTs comparable to the ones obtained using SLO. SHO outperforms Li, giving MFPTs closer to the exact ones over the whole h range considered. Li on the other hand seems to give results which are roughly equivalent to the ones obtained using MT1, MT2, or SLO. For these simulations, the statistical error due to the sample finiteness is of the size of the symbols used.

We would like to note that the numerical experiments were done stretching the algorithms into parameter regions which are somehow extreme: the typical time scale for the potential considered is around 0.5 [the oscillation frequency around the minima for Eq. (13)] or around 1 [the larger γ considered, and the oscillation frequency for the potential of Eq. (14)], and yet an algorithm like SHO is able to integrate

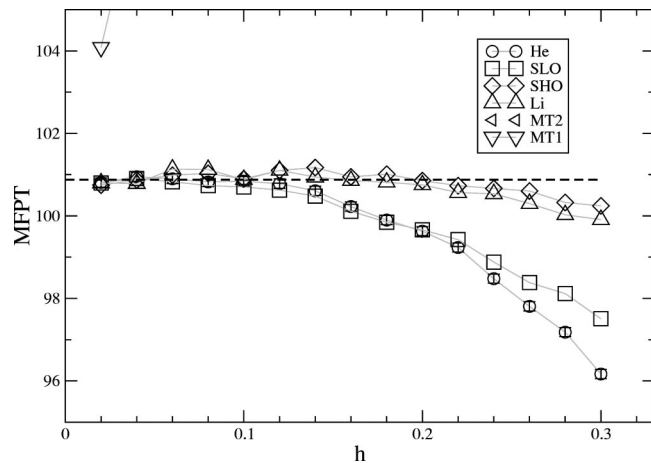


FIG. 5. Result of simulations for different integration schemes, as a function of the integration time step h , for the system in Eq. (13). The mean first passage time between the minima is considered (see text for details), taking $T=0.1$ and $\gamma=1$. The results for MT2 fall outside the figure bounds, and only one point for MT1 is within the bounds. Number of averages used to compute each point in the figure is in excess of 7×10^4 .

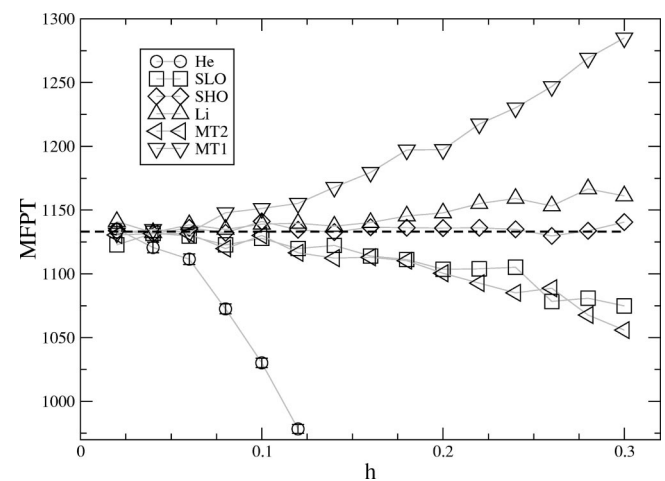


FIG. 6. Result of simulations for different integration schemes, as a function of the integration time step h , for the system in Eq. (13). The mean first passage time between the minima is considered (see text for details), taking $T=0.1$ and $\gamma=10^{-2}$. The number of averages used to compute each point in the figure is in excess of 7×10^3 .

up to integration time steps h order of 0.3, with corrections to the moments or to the MFPT's which are smaller than, or at worse order of, 1 %: in our opinion, these are remarkable results, particularly when the flatness of the MFPT computed with SHO in Fig. 6 is considered.

We should add that comparing algorithms having in mind only the integration time step is only part of the story: for instance, when comparing SHO and Li we should recall that they both require two Gaussian deviates per integration time step, but one (two) evaluation of the deterministic force for Li (SHO), respectively. In all cases (like here) when the stochastic component is computationally heavier than the deterministic component, a comparison like what we did is appropriate (the algorithms take the same time to run). On the other hand, when the deterministic force is the slow part of the simulations (like in the presence of many interacting particles and/or complicated forces), Li will run faster than SHO: at best, Li will be twice as fast as SHO. In this case, we should compare the algorithms in a situation when they take the same time to run: this is easily done via inspection

of the figures, simply stretching the Li data by a factor 2 along the x axis. Even in this case, when the deterministic force dictates the speed of the simulations, for small dampings SHO outperforms Li in the MFPT calculations.

V. CONCLUSIONS

We introduced two algorithms for the numerical integration of the equations of motion of a Brownian walker. The features of these algorithms are that they become symplectic when the damping and the temperature of the Brownian walker are taken to be zero, and give the correct equilibrium distribution to some higher order in the integration time steps for a finite damping and temperature. This, in turn, leads to more accuracy when dynamical quantities are considered (such as MFPT) than leading existing integration schemes. Possible applications of these algorithms are in the integration of the dynamics in the liquid state, where the speed up provided by algorithms which are stable for fairly large time steps may help in improving current simulations.

-
- [1] For a classical introduction, see *Noise in Nonlinear Dynamical Systems*, edited by F. Moss and P. V. E. McClintock (Cambridge University Press, Cambridge, 1989), Vol. 1–3.
 - [2] P. E. Kloeden and E. Platen, *Numerical Simulation of Stochastic Differential Equations* (Springer-Verlag, Berlin, 1992).
 - [3] J. Garcia-Ojalvo and J. Sancho, *Noise in Spatially Extended Systems* (Springer-Verlag, Berlin, 1999).
 - [4] G. N. Milstein and M. V. Tretyakov, SIAM (Soc. Ind. Appl. Math.) J. Numer. Anal. **34**, 2142 (1997).
 - [5] R. Mannella, Int. J. Mod. Phys. C **13**, 1177 (2002).
 - [6] M. P. Allen and D. J. Tildesley, *Computer Simulation of Liquids* (Oxford University Press, Oxford, 2001).
 - [7] A. C. Brańka and D. M. Heyes, Phys. Rev. E **60**, 2381 (1999).
 - [8] H. A. Forbert and S. A. Chin, Phys. Rev. E **63**, 016703 (2000).
 - [9] Ji Qiang and S. Habib, Phys. Rev. E **62**, 7430 (2000).
 - [10] W. Paul and D. Y. Yoon, Phys. Rev. E **52**, 2076 (1995).
 - [11] J. A. Izaguirre, D. P. Catarello, J. M. Wozniak, and R. D. Skeel, J. Chem. Phys. **114**, 2090 (2001).
 - [12] R. D. Skeel and J. A. Izaguirre, Mol. Phys. **100**, 3885 (2002).
 - [13] W. Wang and R. D. Skeel, Mol. Phys. **101**, 2149 (2003).
 - [14] G. N. Milstein and M. V. Tretyakov, *Numerical Methods for Langevin Type Equations Based on Symplectic Integrators* (Weierstrab-Institut für Angewandte Analysis und Stochastik, Berlin, 2002).
 - [15] G. N. Milstein, Yu. M. Repin, and M. V. Tretyakov, SIAM (Soc. Ind. Appl. Math.) J. Numer. Anal. **40**, 1583 (2003).
 - [16] G. N. Milstein and M. V. Tretyakov, IMA J. Numer. Anal. **23**, 1 (2003).
 - [17] M. Freidlin and A. D. Wentzel, *Random Perturbations in Dynamical Systems* (Springer, New York, 1984).
 - [21] G. G. Batrouni, G. R. Katz, A. S. Kronfeld, G. P. Lepage, B. Svetitsky, and K. G. Wilson, Phys. Rev. D **32**, 2736 (1985).
 - [18] H. Yoshida, Phys. Lett. A **150**, 262 (1990).
 - [19] J. M. Sanz-Serna, Acta Numerica **1**, 243 (1991).
 - [20] R. Mannella, in *Supercomputation in Nonlinear and Disordered Systems*, edited by L. Vasquez, F. Tirado, and I. Martin (World Scientific, Singapore, 1997), pp. 100–129.
 - [22] C. M. Luscher, Comput. Phys. Commun. **79**, 100 (1994).
 - [23] F. James, Comput. Phys. Commun. **79**, 111 (1994).
 - [24] G. Marsaglia and W. W. Tsang, SIAM (Soc. Ind. Appl. Math.) J. Sci. Stat. Comput. **5**, 349 (1984).